# THERMAL FIELD ANALYSIS FROM THE TURBO-GENERATOR ROTOR WITH DIRECT COOLING

Nicolae Voicu, Mihai Iordache

*"Politehnica" University of Bucharest, Electrical Engineering Department,*
*Spl. Independentei 313, Cod 06 0042, Bucharest ROMANIA,*
*Phone/Fax (+401) 411 11 90 iordache@hertz.pub.ro*

*Our paper presents a combined method for the steady-state thermal field analysis from the turbo-generator rotor with the direct cooling. The thermal field analysis is made in two stages: 1) In the first stage, in order to determine the domain with the highest temperature, the thermal field is simulated by the thermal resistances and concentrated losses; 2) In the second stage, using the 3D finite difference method, we determine with a very good accuracy the point with the highest temperature from the rotor.*

## 1. INTRODUCTION

We assume that the turbo-generator rotor is directly cooled, and the cooling agent (the air) is directed towards the rotor active parts, avoiding in the most part the temperature fall in the isolated layer. The analysis method of the thermal field presented in [1, 3] can determine only one temperature value for each surface which delimit the considered subdomain. In this way, the thermal field analysis, for the most thermal solicited subdomain, can be computed with the adequate accuracy by the 3D finite difference method.

In our paper, the used method for the selection of the most thermal solicited subdomain permits the determination of a more accuracy distribution of the thermal field on the subdomain delimitated surfaces. Thus, the 3D finite difference method is much more accuracy. Modelling the thermal field by the thermal resistances and concentrated losses we obtain an equivalent large-scale nonlinear resistive circuit. This nonlinear circuit is analysed by an original hybrid method. If the nonlinear resistive circuit contains time-dependent sources it will be analysed by repeating the hybrid analysis at different instants of time.

The hybrid equations were automatically formulated in the symbolic or partially symbolic and they were performed by using the ECSAP – Electronic Circuit Symbolic Analysis Program [7]. ECSAP is based on the modified nodal method in the symbolic form. It is written in C++ language and it was implemented on the compatible IBM Pentium PC.

## 2. ANALYZED PHYSICAL MODEL

Because, the turbo-generator rotor has a cylindrical symmetry, we have chosen a portion of the rotor delimitated as in Fig.1. This domain includes the slot in which there are the copper bar and iron adjacent parts. In order to analyze the thermal field by the thermal resistances and concentrated losses method, the physics model was partitioned in 16 subdomains as in Fig. 2. A subdomain is delimited by the following planes: the planes passing through the symmetric axes between two successively ventilation slots (these axes are rectangular on the longitudinal rotor axis), the median rotor bar plane, and the tooth rotor median plane (Fig. 2).

Because the thermal transfer towards the rotor shaft is neglected in the modelling process, the iron portion from the rotor bar bottom does not taken consideration. But, in the 3D finite difference analysis the chosen subdomain will contain and this neglected portion.

For each subdomain the boundary conditions are:

*T* is independent on the axial coordinate;

$\frac{\partial T}{\partial n} = 0$, for the boundaries delimitated by the following planes: the symmetrical plane of the rotor bar, the plane of symmetry corresponding to the rotor tooth, and the armature rotor surface towards the shaft;

$\lambda \frac{\partial T}{\partial n} + \alpha(T - T_e) = 0$, for all ventilated surfaces, where: $T$ – is the surface temperature, $T_e$ – represents the air temperature in the surface neighbourhood, $\lambda$ - is the heat transfer coefficient by conduction, and $\alpha$ - represents the heat transfer coefficient by convection.

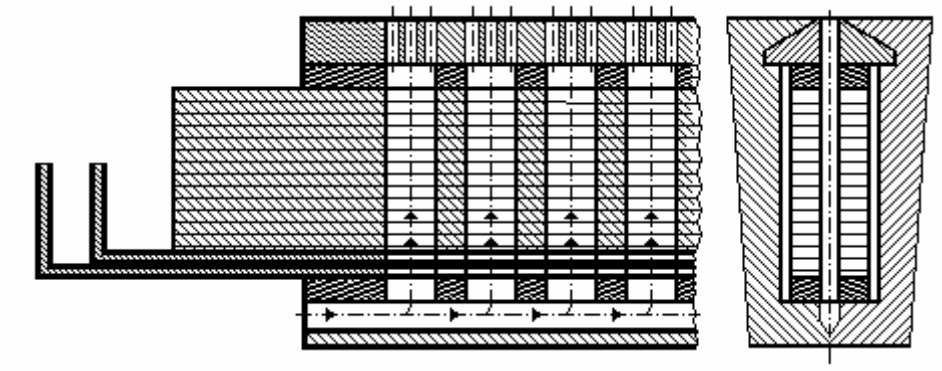

Fig.**1**. Analyzed physical model.

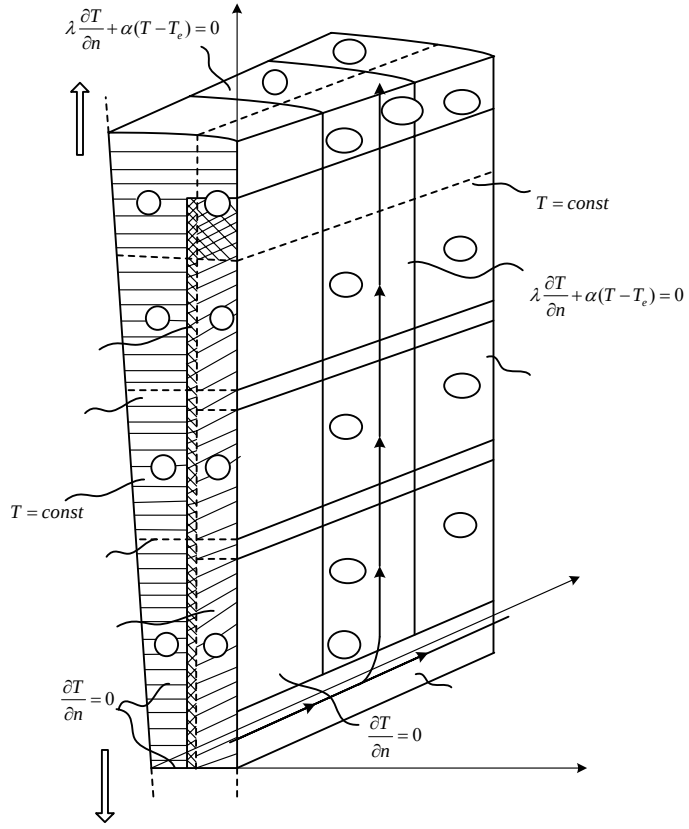


Fig.**2.** Analyzed subdomain.

## 3. THERMAL FIELD MODELING BY THERMAL RESISTANCES AND COCENTRATED LOSSES

Tacking into account the heat transfer types and the analogy between the electrical circuits and thermal networks in [4] is presented the modelling principle of the thermal field by the thermal resistances and concentrated losses. For the subdomain shown in Fig. 2, the

equivalent electrical circuit associated to the thermal field simulation by the thermal resistances and concentrated losses is presented in Fig. 3.

The circuit elements in Fig. 3 have the following physics signification:

- resistors correspond to the heat transfer by the conductivity and by convection;
- ideal independent voltage sources correspond to the cooling agent temperatures;
- ideal independent current sources correspond to the losses in copper.

An equivalent electric circuit as in Fig. 3 containing the same circuit elements, but having the different values simulates each of the 16 subdomains of the analyzed model.

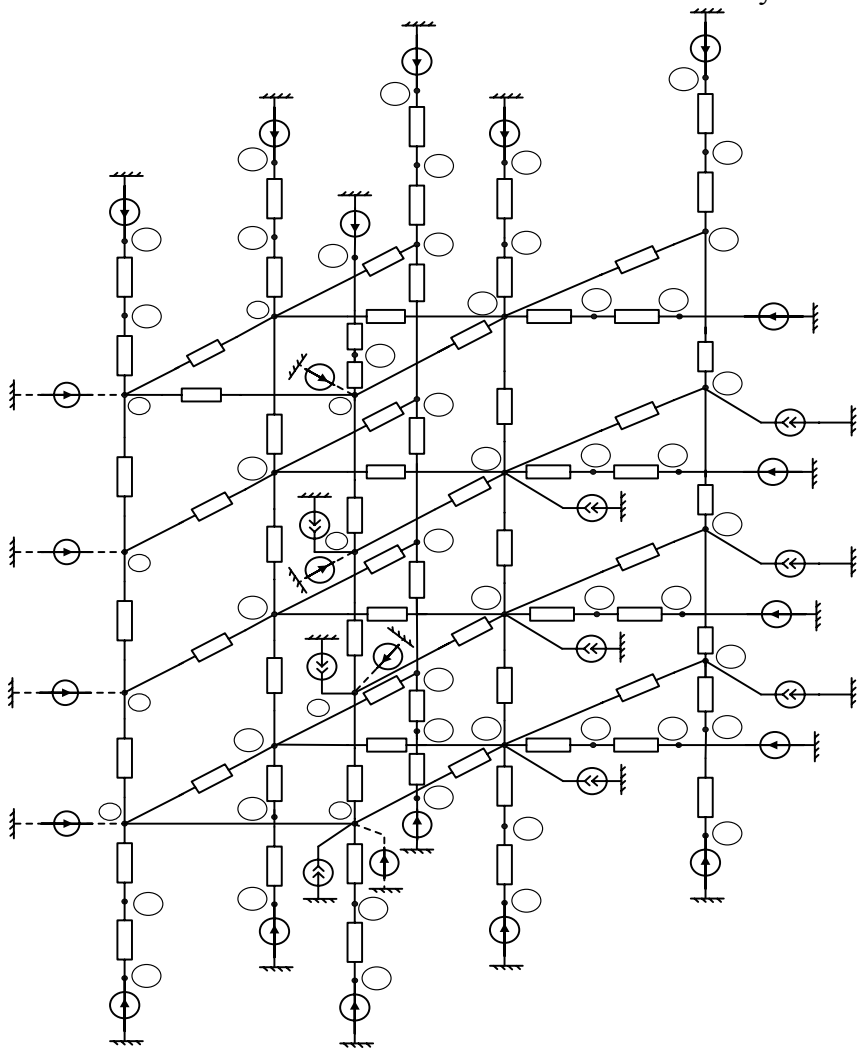

Fig.**3.** Equivalent electrical network.

The equivalent network for the whole-analysed domain is obtained by the cascade connection of the equivalent circuits of the 16 subdomains. The air warming in the axial air path is neglected, so that the equivalent voltage sources corresponding to the air temperature have the same value. The air warming $\Delta T_a$ along the radial ventilation slot is considered linear one (Fig. 4), its value is determined through a thermal balance, considering the air flow through the slot and the evacuated losses as being known.

The equivalent resistive circuit represented in Fig. 3 was analysed by the circuit simulator program ECSAP – Electronic Circuit Symbolic Analysis Program [7]. PMNA is based on the modified nodal analysis of the linear or/and nonlinear electric circuits [2, 5]. This method is associated to the original algorithm based on the *node tearing*, in which the subcircuits are torn apart along appropriate nodes [2, 4, and 8]. Node tearing method leads to a bordered block-diagonal form of the circuit matrix. The development of the parallel processing system

for solving a number of circuits simultaneously leads to a reduction in computation time and to an increase of the accuracy.

The air warming $\Delta T_a$ along the radial ventilation slot is considered linear one (Fig. 4), its value is determined through a thermal balance, considering the air flow through the slot and the evacuated losses as being known.

The equivalent resistive circuit represented in Fig. 3 was analysed by the circuit simulator program ECSAP – Electronic Circuit Symbolic Analysis Program [7]. PMNA is based on the modified nodal analysis of the linear or/and nonlinear electric circuits [2, 5]. This method is associated to the original algorithm based on the *node tearing*, in which the subcircuits are torn apart along appropriate nodes [2, 4, and 8]. Node tearing method leads to a bordered block-diagonal form of the circuit matrix. The development of the parallel processing system for solving a number of circuits simultaneously leads to a reduction in computation time and to an increase of the accuracy.

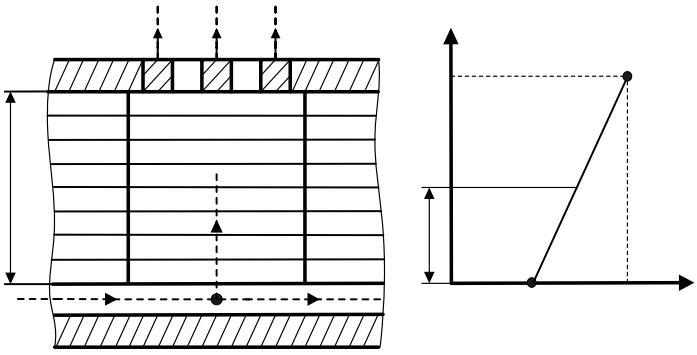

Fig.**4.** Air warming along the radial slot.

## 4. THE HEAT TRANSFER COEFFICIENT THROUGH CONVECTION

For a better determination of the α coefficient, experimental determinations have been made on a physical model with a rotor notch of a turbo-generator on the 1:1 scale, processing results allowing a generalisation for electrical machines with similar ventilation systems.

According to the “theory of similitude”, the solution of the differential equation for the thermal convection can be put in criteria equations like:

$$N_u = f\left(R_e, P_r\right), \tag{1}$$

where:

$N_u = \frac{\alpha d_e}{\lambda}$ - is the Nusselt criteria; $R_e = \frac{v d_e}{\nu}$ - the Reynolds criteria; $P_r = \frac{\nu c \gamma}{\lambda}$ - the Prandtl criteria.

For the stationary regime, if the cooling fluid is forced to flow, equation (1) is like:

$$CR_e^m = \frac{N_u}{P_r^n}, \tag{2}$$

where *C, m, n* are determined experimentally.

The processing of the results determines eventually the *C, m, n* constants, as well as the correlation constant $K = CR_e^m$, depending on the $R_e$ criteria and other fluids ($H_2$, for example).

So, for the radial ventilation slots, the correlation coefficient is:

$$K = 0.0031\ R_e^{1,5073} \tag{3}$$

and the values of the same coefficient, when dealing with smooth pipes:

$$K_0 = 0{,}0023\ R_e^{1,5072} \tag{4}$$

The value of *m* coefficient is determined experimentally and is $m = 0.43$.

The (2) equation for the system's ventilation slots:

$$0{,}0031R_e^{1,5073} = \frac{N_u}{P_r^{0,43}} = K \tag{5}$$

For the system's ventilation slots, the heat transfer coefficient through convection $\alpha(z, Ta)$ depends on the position $z$ and the temperature of the cooling fluid and is obtained using the following algorithm:

1. Calculate $R_e$;
2. Get the value of the correlation coefficient $K$ using (3);
3. Knowing the flow rate balance of the cooling fluid in the slots, calculate the speed of the air;
4. Calculate the air temperature $T_a(z)$;
5. Obtain the $\alpha$ coefficient from (5).

## 6. MODELING OF THE THERMAL FIELD FROM THE MOST USED SUBDOMAIN, USING THE 3D FINITE DIFFERENCE METHOD

Analysing the equivalent network corresponding to the thermal field of the analysed domain resulted that the first subdomain is the most used, thermally.For a better (more precise) determination of the thermal distribution one can use "the 3D finite difference method".

The internal (Fourier) thermal conductivity equation for a Σ boundary surface is:

$$\lambda \int_{\Sigma} gradTndA = P_{\Sigma} \tag{6}$$

For the interior domain (Fig. 5), by discretising the (6) equation the following is obtained:

$$\lambda_I \frac{T_0 - T_1}{\Delta y_1} \frac{\Delta x_5}{2} \frac{\Delta z_3}{2} + \lambda_{II} \frac{T_0 - T_1}{\Delta y_1} \frac{\Delta z_6}{2} \frac{\Delta x_5}{2} + \ldots$$
$$+ \lambda_{VIII} \frac{T_0 - T_3}{\Delta z_3} \frac{\Delta x_2}{2} \frac{\Delta y_4}{2} = P_{\Sigma}, \tag{7}$$

where $\lambda_I, \lambda_{II}, \lambda_{VIII}$ are the thermal conductivities of the subdomains after the partitioning.

The (7) equation can be put like this:

$$(T_0 - T_1)\Lambda_1 + (T_0 - T_2)\Lambda_2 + (T_0 - T_3)\Lambda_3 + (T_0 - T_4)\Lambda_4 + (T_0 - T_5)\Lambda_5 + (T_0 - T_6)\Lambda_6 = P_{\Sigma}. \tag{8}$$

where:

$\Lambda_1, \Lambda_2, \Lambda_6$ are coefficients like:

$$\Lambda_I = \frac{\lambda_I \Delta x_5 \Delta z_3 + \lambda_{II} \Delta x_5 \Delta z_6 + \lambda_{III} \Delta x_2 \Delta z_3 + \lambda_{IV} \Delta z_6 \Delta x_2}{4 \Delta y_1}.$$

The (8) equation is valid only for the points from interior of the Σ domain.

For mixed boundary surfaces (Fig. 6), the Fourier equation is like:

$$-\lambda \frac{\partial T}{\partial n} + \frac{T_1 - T_2}{\Delta_2} \lambda S_2 + \frac{T_1 - T_7}{\Delta_7} \lambda S_7 + \frac{T_1 - T_4}{\Delta_4} \lambda S_4 +$$
$$+ \frac{T_1 - T_3}{\Delta_3} \lambda S_3 + \frac{T_1 - T_6}{\Delta_6} \lambda S_6 = P_{\Sigma}. \tag{9}$$

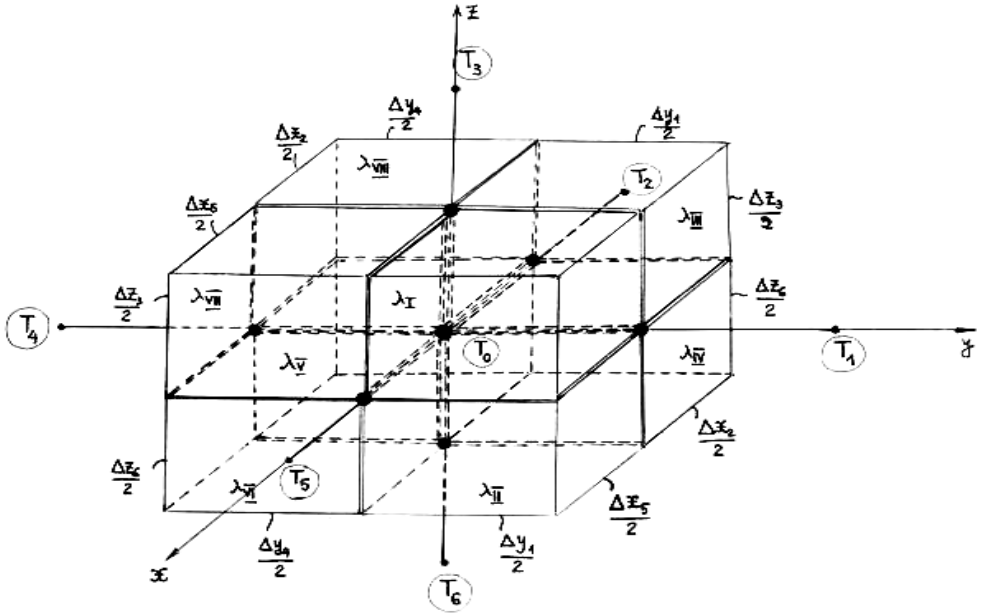


Fig.**5.** The discreting subdomains.

Because

$$\lambda \frac{\partial T}{\partial n} + \alpha\left(T - T_e\right) = 0 \tag{10}$$

the equation (9) becomes:

$$\begin{aligned} &\alpha(T - T_e) + \frac{T_1 - T_2}{\Delta_2}\lambda S_2 + \frac{T_1 - T_7}{\Delta_7}\lambda S_7 + \\ &+ \frac{T_1 - T_4}{\Delta_4}\lambda S_4 + \frac{T_1 - T_3}{\Delta_3}\lambda S_3 + \frac{T_1 - T_6}{\Delta_6}\lambda S_6 = P_\Sigma . \end{aligned} \tag{11}$$

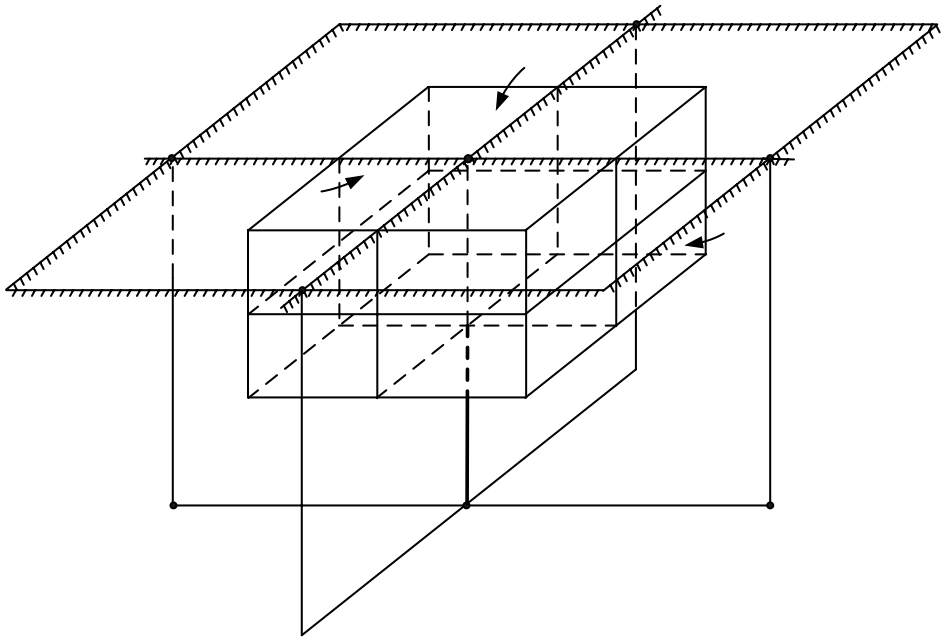

Fig. **6.** Mixed boundary conditions.

To resolve the algebraic system obtained through discretising the Fourier equation in all the subdomains after the partitioning, the mixed boundary condition must be a Dirichlet condition.Therefore, the mixed boundary surface doubles by mirroring itself with the δrange and the space between has the $\lambda_f$ conductivity (Fig. 7), which is determined from the real and doubled surfaced equation transfers with the following Fourier equation:

$$\begin{aligned}&\frac{T_1-T_e}{\delta}\lambda_f S_e+\frac{T_1-T_2}{\Delta_2}\lambda(S_2+\delta\Delta x)+\\&+\frac{T_1-T_7}{\Delta_7}(S_7+\delta\Delta y)+\frac{T_1-T_3}{\Delta_3}\lambda(S_3+\delta\Delta x)+\\&+\frac{T_1-T_3}{\Delta_3}\lambda(S_3+\delta\Delta x)+\frac{T_1-T_6}{\Delta_6}\lambda(S_6+\delta\Delta y)=P_\Sigma.\end{aligned} \tag{12}$$

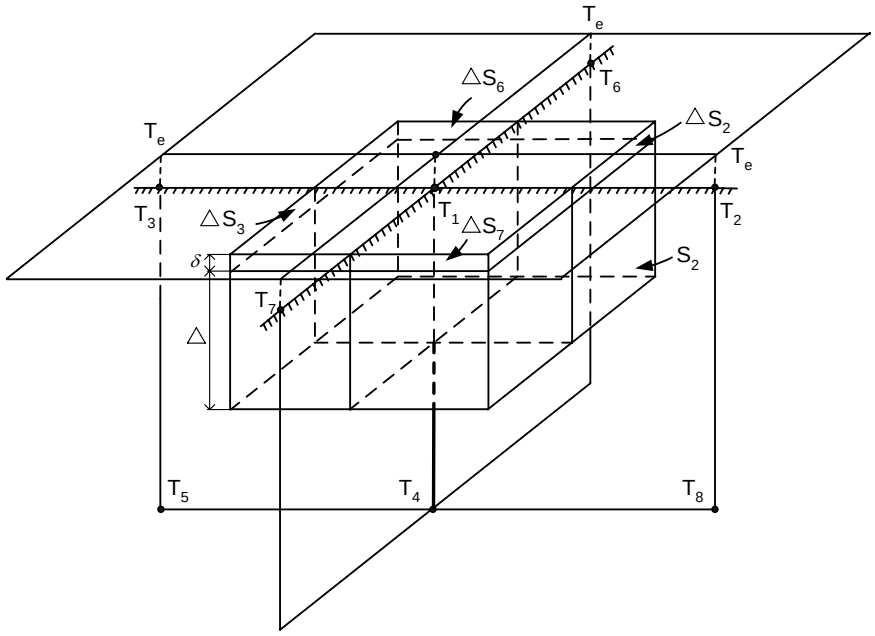


Fig.**7.** Boundary element with doubled surface.

Because the equation (9) is equivalent to the equation (11), it results:

$$\lambda_f=\frac{\alpha\delta}{S_e} \tag{13}$$

**Remarks:**

1. When δ –>0, by keeping the (10) condition, the (11) equation becomes (9);
2. The $\lambda_f$ conductivity proportionally decreases itself with of the reduction of the δ thickness. The heat transfer on the z axis is preserved, instead the transfers on the x and y axes squarely decrease with the reduction of δ;
3. The algorithm is valid even for interior surfaces, which divide different conductivity environments.

## 7. CONCLUSIONS

The presented method allows the selection of the most thermal stressed through the thermal resistance method and then a more precise determination of the subdomain thermal field (above 100 points) through the 3D finite difference method;

By analysing the equivalent electrical network, the head area of the copper bar (first subdomain) seemed to be the most thermal stressed, and this because of the larger free spaces where the airflow can not be totally controlled. The thermal distribution of the height of the

copper bar for the first subdomain and the experimental values obtained on the physical model are presented in Fig. 8.

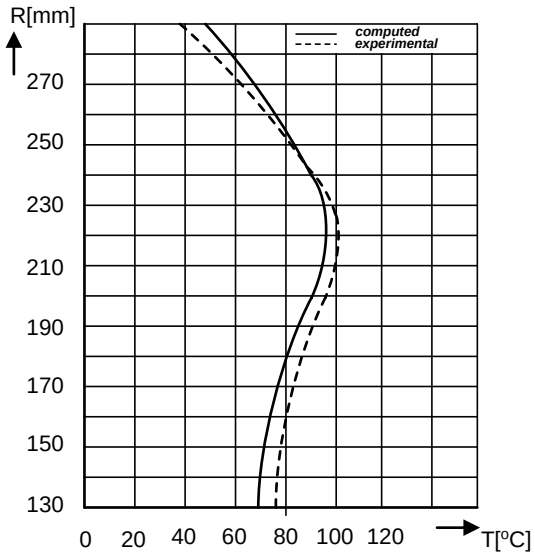


Fig. **8.** Thermal distribution of the height of the copper bar for current density in rotor copper $J$= 3.88 [A/mm$^2$], and cooling airflow $D$=3.35 [Nm$^3$/h].

The possibility of the determination of the thermal field by the rotor bars of the turbo - generator with direct cooling, by use, for each subdomain, of a 3D network with a great number of nodes, leads to establishing the points with the great temperatures and taking corresponding protection steps. The diakoptic approach leads to a significant reduction of CPU time and an important economy of memory, in contrast with the case when the analysis is made over the entire circuit. When the symbolic analysis of the whole large-scale circuit is not possible, the tearing method becomes the unique alternative and this is its main advantage.

## 8. REFERENCES

[1] G. Galasso, "Opttimizzatione del reffreddamento di turboalternatori", *Elettrotecnica*, (1987), pp. 7 - 14;

[2] M. Iordache, "An efficient algorithm for tearing large - scale networks", *Rev. Roum. Sci. Techn. - Electrotechn. et. Energ.*, vol. **2**, pp. 203 – 209 (1990).

[3] A. C. Williamson, "Measurement of rotor temperatures of a 500 MW turbine generator with un balanced loading", *Proc. IEE*, vol. **8**, pp. 795 – 803 (1976).

[4] M. Iordache, N. Voicu, "Thermal Resistance Modelling of the Heating of Convection Cooled Turbo-Generator Rotors", *Modelling, Measurement & Control*, *AMSE Press*, No**. 2**, pp. 45-54 (1994).

[5] M. Iordache, M. Perpelea, "Modified nodal analysis for large-scale piecewise-linear nonlinear electric circuits", *Rev., Roum., Sci., Techn., Électrotechn. et Énerg*., vol. **4**, pp. 487-496 (1992).

[6] M. Iordache, N. Voicu, "A Method for Thermal Field Determination in Turbo-Generator Rotors with Direct Cooling", in *Proccedings Part 2 of International Conference on the Evolution and Modern Aspects of Synchronous Machines Zurich, Switzerland, 27-29 August,* pp. 580-586 (1991).

[7] M. Iordache, Lucia Dumitriu, *ECSAP – Electronic Circuit Symbolic Analysis Program*, Department of Electrical Engineering, Bucharest (2002);

[8] A.F. Schwartz, Computer-aided design of microelectronic circuits and systems, Academic Press, London, 1987.